Annals of Biomedical Engineering, Vol. 38, No. 3, March 2010 *(© 2010)* pp. 1048–1059
DOI: 10.1007/s10439-009-9874-z

Baseline Characteristics of Dual-Axis Cervical Accelerometry Signals

ERVIN SEJDIĆ,[1] VICKI KOMISAR,[2] CATRIONA M. STEELE,[3] and TOM CHAU[1]

[1]Bloorview Research Institute, Bloorview Kids Rehab and the Institute of Biomaterials and Biomedical Engineering, University of Toronto, Toronto, ON, Canada; [2]Department of Engineering Science, University of Toronto, Toronto, ON, Canada; and [3]Toronto Rehabilitation Institute and the Department of Speech-Language Pathology, University of Toronto, Toronto, ON, Canada

(Received 2 May 2009; accepted 9 December 2009; published online 16 January 2010)

Associate Editor Sean S. Kohles oversaw the review of this article.

Abstract—Dual-axis swallowing accelerometry is a promising noninvasive tool for the assessment of difficulties during deglutition. The resting and anaerobic characteristics of these signals, however, are still unknown. This paper presents a study of baseline characteristics (stationarity, spectral features, and information content) of dual-axis cervical vibrations. In addition, modeling of a data acquisition system was performed to annul any undesired instrumentation effects. Two independent data collection procedures were conducted to fulfil the goals of the study. For baseline characterization, data were acquired from 50 healthy adult subjects. To model the data acquisition (DAQ) system, ten recordings were obtained while the system was exposed to random small vibrations. The inverse filtering approach removed extraneous effects introduced by the DAQ system. Approximately half of the filtered signals were stationary in nature. All signals exhibited a level of statistical dependence between the two axes. Also, there were very low frequency oscillations present in these signals that may be attributable to vasomotion of blood vessels near the thyroid cartilage, blood flow, and respiration. Demographic variables such as age and gender did not statistically influence baseline information-theoretic signal characteristics. However, participant age did affect the baseline spectral characteristics. These findings are important to the further development of diagnostic devices based on dual-axis swallowing vibration signals.

Keywords—Dual-axis swallowing accelerometry signals, Baseline, Auto-regressive modeling, Stationarity, Information-theoretic analysis.

INTRODUCTION

The current gold standard for detection and management of dysphagia (swallowing difficulty) is based on the videofluoroscopic swallowing study (VFSS).[25] Despite its effectiveness, VFSS is not suitable for day-to-day monitoring because of long waiting lists and excessive exposure to ionizing radiation.[39,47] An alternative approach for a noninvasive assessment of swallowing disorders is swallowing accelerometry,[41,40] a technique that involves an accelerometer placed on the neck to monitor vibrations associated with swallowing activities. Although single-axis accelerometers were traditionally used,[7,12,19,42] recent contributions showed that dual-axis accelerometers yield more information and enhance analysis capabilities,[20,46] likely because of the two-dimensional movement of the hyoid and the larynx during swallowing.[18,15]

Even though accelerometry is becoming a valuable technique for the assessment of swallowing difficulties, some fundamental issues remain unaddressed. First, the baseline characteristics of such signals have not been studied. For example, baseline stationarity and the baseline relationship between signals in the anterior–posterior (A–P) and superior–inferior (S–I) directions are currently unknown. Answers to these questions are critical to the further development of diagnostic devices based on dual-axis swallowing vibration signals. Second, while the nonidealities in data acquisition (DAQ) systems may alter swallowing characteristics, these effects have not been studied nor mitigated to date.

The main contribution of this paper is the inaugural analysis of baseline characteristics of dual-axis accelerometry signals obtained from 50 consenting healthy adults. In particular, we examine several statistical features, including stationarity, entropy rate, and mutual dependence between the two axes. These features have not been previously examined for the dual-axis cervical vibration signals in the absence of swallows. To isolate baseline cervical vibrations, we model the employed DAQ system using a general autoregressive (AR) approach.

Address correspondence to Ervin Sejdić, Bloorview Research Institute, Bloorview Kids Rehab and the Institute of Biomaterials and Biomedical Engineering, University of Toronto, Toronto, ON, Canada. Electronic mail: esejdic@ieee.org, v.komisar@utoronto.ca, steele.catriona@torontorehab.on.ca, tom.chau@utoronto.ca

METHODOLOGY

Mathematical Background

This paper deals with signals acquired by a dual-axis accelerometer. To simplify notation and avoid repetition, the formulations in this section are based on a signal acquired from a single axis only, but apply equally to signals from both axes.

Autoregressive Modeling of Data Acquisition System

Under the assumption that a system can be characterized by a rational structure, a signal can be modeled as an output of such a system using parametric methods.[16] More precisely, the parameters of a model are evaluated based on the samples of the acquired signal, $x(n)$, of length N, where $0 \le n \le N-1$. Among various modeling techniques, AR-based modeling methods are often used since the AR parameters can be easily estimated by solving linear equations,[29,32] unlike the estimation of AR-moving-average or moving-average parameters, which require solving a set of nonlinear equations.[16] The AR method models data, $x(n)$, as output of a causal, all-pole, discrete filter of order q whose input is white Gaussian noise[16,29,32]:

$$x(n) = -\sum_{r=1}^{q} a_r x(n-r) + w(n), \tag{1}$$

where a_r is the AR coefficients and $w(n)$ is the white Gaussian noise with variance σ^2. Thus, a complete AR model consists of the filter coefficients $\{a_1, a_2, ..., a_q\}$ and the variance σ^2 of the driving noise process $w(n)$ (compactly represented by a real-valued parameter vector $\theta = [\sigma^2, a_1, a_2, ..., a_q]$).

Different approaches exist to evaluate the AR parameters of (1), and for an in-depth review, the reader is referred to classical references by Kay,[16] Kay and Marple,[17] and Marple,[28] In this paper, the so-called modified covariance method is used for system modeling,[27,28] as it avoids drawbacks (e.g., estimation bias and line splitting) associated with other well known methods such as Burg's method and the Yule–Walker technique.[27] The modified covariance method minimizes the average of the forward and backward linear prediction errors. For full details of the algorithm, please refer the studies by Kay,[16] and Marple.[27,28]

The modified covariance approach yields the unknown AR parameters (i.e., θ), but we still need to estimate the unknown length of the vector θ, i.e., to select the appropriate model order.[24] In this paper, the Bayesian information criterion (*BIC*) is used to determine the model order[45]:

$$BIC(Q) = -2\ln p\left(x\middle|\widehat{\theta}, Q\right) + Q\ln N, \tag{2}$$

where Q is the length of the vector $\widehat{\theta}$ with $\widehat{\theta}$ being the maximum likelihood estimate of θ and $p(x|\widehat{\theta}, Q)$ is the likelihood of the observed data x given $\widehat{\theta}$ and Q. The model order is found by minimizing the above equation. The BIC yields a more concise description of a system[3] in comparison to Akaike information criterion (AIC).[1] Moreover, BIC provides more consistent results than AIC, that is, the probability of correct detection approaches unity as $N \to \infty$ as long as the data-generating mechanism belongs to the model class considered.[48,51] Note that in using an approach based on the minimum description length (MDL), BIC can be obtained.[43]

Statistical Characterization of Dual-Axis Cervical Accelerometry Signals

The previous section outlined the methodology for the characterization of the DAQ system. In this section, we describe the methods used to characterize the baseline behavior of dual-axis swallowing vibration signals. We can consider $x(n)$ (defined above) to be a discrete-time series since the observations are made at a discrete set of times, Υ, where the cardinality of Υ is N.[5] This time series is then a realization of the family of real-valued random variables $\{\chi_n, n \in \Upsilon\}$ that are considered to be a stochastic process defined on a probability space.[5]

Stationarity test. Stationarity is a property of a time series in which the probability distribution of values of the series are independent of time translations.[4,5,33] Specifically, a time series is strictly stationary if the cumulative distribution function of the joint distribution, $F_{\chi_1,\ldots,\chi_N}(x_1, x_2, \ldots, x_N)$, is invariant to a shift in the origin, i.e.,

$$F_{\chi_1,\ldots,\chi_N}(x_1, x_2, \ldots, x_N) = F_{\chi_{1+\tau},\ldots,\chi_{N+\tau}}(x_1, x_2, \ldots, x_N) \tag{3}$$

for all positive τ.[33] This is also referred to as a strong stationarity, as opposed to weak or wide-sense stationarity, in which only the first two moments of the series are required to be time-invariant[4,33]:

$$E\{\chi_\varepsilon\} = E\{\chi_{\varepsilon+\tau}\} \tag{4}$$

$$\mathrm{Cov}(\chi_\varrho, \chi_\varsigma) = \mathrm{Cov}(\chi_{\varrho+\tau}, \chi_{\varsigma+\tau}), \tag{5}$$

where $\varepsilon, \varrho, \varsigma \in \Upsilon$. The stationarity of a time series can be assessed with the reverse arrangement test, a nonparametric approach for determining weak or wide-sense stationarity of a time series.[4] It has been applied in several fields,[2,6] including the analysis of swallowing vibration signals.[7,19,20] The following steps can thus be

taken to analyze the stationarity of a time series with the reverse arrangement test[4,7]:

1. Divide the time series into K nonoverlaping segments, with the assumption that the data within each segment is independent. If the length of a segment is known, then the number of segments can be calculated as

$$K = \left\lfloor \frac{N}{L} \right\rfloor, \tag{6}$$

where L is the desired segment length and $\lfloor \bullet \rfloor$ represents the greatest integer function. It is noted that N is not necessarily an integer multiple of K, making it necessary to omit some of the data points. Previous research on swallowing signals showed that there are no significant statistical differences between various approaches to data trimming.[7] Therefore, the data will be trimmed from both sides as suggested by Chau *et al.*,[7] and the trimmed version of the signal is denoted by $x_{tr}(m)$, where $0 \le m \le M-1$ and $M = KL \le N$.

2. Form a vector $y \in \mathbb{R}^K$ of mean square values whose points are assigned as follows:

$$y(k) = \frac{1}{L} \sum_{j=kL}^{(k+1)L-1} x_{tr}^2(j) \quad \text{for } 0 \le k \le K-1. \tag{7}$$

3. A reverse arrangement occurs when $y(a) > y(b)$ for $a < b$. Using this rule, an indicator sequence, ω, for $y(k)$ can be formed:

$$\omega(d) = \begin{cases} 1 & \text{if } y(k) > y(l) \text{ for } k < l \\ 0 & \text{otherwise} \end{cases} \tag{8}$$

for $k+1 \le l \le K-1$, $1 \le d \le D$ where $D = K-k-1$. Therefore, the number of reverse arrangements for kth value is given by

$$\xi(k) = \sum_{d=1}^{D} \omega(d) \tag{9}$$

and the total number of reverse arrangements is given by

$$\Omega = \sum_{k=0}^{K-1} \xi(k). \tag{10}$$

4. For a stationary time series, the distribution of Ω is approximately normal and its expected value is given by Chau *et al.*[7]

$$\mu_\Omega = \frac{L(L-1)}{4} \tag{11}$$

and its variance by

$$\sigma_\Omega^2 = \frac{L(L-1)(2L+5)}{72}. \tag{12}$$

Therefore, the null hypothesis is that Ω comes from a normal distribution with its mean and variance given by (11) and (12), respectively. The null hypothesis is rejected at a significance level α if Ω falls outside the corresponding critical values.

In this paper, the test statistic

$$\rho_\Omega = \frac{\Omega - \mu_\Omega}{\sigma_\Omega} \tag{13}$$

was used, with the assumption that $\rho_\Omega \sim \mathcal{N}(0, 1)$.[7] The critical values at significance level α are then $\rho_{1-\alpha/2}$ and $\rho_{\alpha/2}$ where ρ is a standard normal variate, and for a 5% significance level these are given by $\rho_{\alpha/2} = -1.96$ and $\rho_{1-\alpha/2} = 1.96$. The values of the test statistics, ρ_Ω, can fall within one of the three possibilities:

- $\rho_\Omega \le \rho_{\alpha/2}$—There are fewer reverse arrangements than expected of a stationary signal, implying the presence of an upward trend in the mean square sequence.
- $\rho_\Omega \ge \rho_{1-\alpha/2}$—There are more reverse arrangements than expected of a stationary signal, implying that a downward trend is present in the mean square sequence.
- $\rho_{\alpha/2} < \rho_\Omega < \rho_{1-\alpha/2}$—The null hypothesis that a time series is (weakly) stationary can be accepted.

Characterization using information-theoretic measures. Our next concern is the amount of information carried by these time series. Since we are dealing with random processes, we estimate the entropy and information rates[11] based on the estimation of conditional entropies.[34–37] The complete review of the approach is beyond the scope of this manuscript, and only the key steps are presented here.

As the first step, we normalize the time series, $x(n)$, to zero mean and unity variance:

$$X(n) = \frac{x(n) - \mu_x}{\sigma_x}, \tag{14}$$

where μ_x and σ_x represent the sample mean and standard deviation, respectively. The normalized time series, $X(n)$, is then transformed into a sequence of symbols, $X_\lambda(n)$, by using λ quantization levels and a limited alphabet $\{0, 1, \ldots, \lambda-1\}$. As the next step, patterns of W delayed samples are constructed as: $X_{\lambda_W}(n) = \{X_\lambda(n), X_\lambda(n-1), \ldots, X_\lambda(n-W+1)\}$. Using the predefined patterns, $X_{\lambda_W}(n)$, the conditional entropy is then defined as[36]:

$$H_{cond}(\lambda, W) = -\sum p[X_{\lambda_{W-1}}] \sum p[X_\lambda(n)|X_{\lambda_{W-1}}] \log p[X_\lambda(n)|X_{\lambda_{W-1}}], \tag{15}$$

where $p[X_{\lambda_W}]$ is the probability of the pattern X_{λ_W} and $p[X_\lambda(n)|X_{\lambda_{W-1}}]$ is the probability of the pattern $X_\lambda(n)$ when the previous $W-1$ patterns are given. Equation (15) can be simply calculated using the following[34–37]:

$$H_{cond}(\lambda, W) = H(\lambda, W) - H(\lambda, W-1), \quad (16)$$

where $H(\lambda, W)$ is the Shannon entropy. $H_{cond}(\lambda, W)$ measures the regularity with which patterns follow each other in the time series, whereas Shannon entropy measures the incidence of the patterns in the time series. Equation (15) can lead to numerical instabilities, and therefore, a corrected $H_{cond}(\lambda, W)$ has been proposed[34]:

$$H_{corr}(\lambda, W) = H_{cond}(\lambda, W) + H(1, W)\Xi(\lambda, W), \quad (17)$$

where $\Xi(\lambda, W)$ is the percentage of the patterns occurring only once in the series. Furthermore, by normalizing $H_{corr}(\lambda, W)$ by $H(1, W)$, we obtain the normalized corrected conditional entropy, $H_{norm}(\lambda, W)$ ranging from zero to one. The minimum of $H_{norm}(\lambda, W)$ may be useful for the comparison of processes with different probability distributions,[37] which might be the case with signals considered in this paper. Hence, a so called index of regularity has been proposed[37]:

$$\varrho = 1 - \min\left(H_{norm}(\lambda, W)\right). \quad (18)$$

The index ranges from zero, denoting maximum complexity, to one denoting maximum regularity. In other words, if the time series is highly predictable (e.g., sinusoid), the index of regularity is close to one, while for the time series representing white Gaussian process, the index is close to zero.

The index of regularity provides information about a single time series. We are also interested in the coupling (or synchronization) between two time series. Following similar derivations as above, one can arrive at a synchronization index, η, the degree of uncoupling between two time series[35]:

$$\eta = 1 - \min\left(\Gamma_{x|y}(W)\right), \quad (19)$$

where $\Gamma_{x|y}(W)$ is the estimate of the so-called uncoupling function. This synchronization index exploits the fact that the conditional entropy between two signals reflects the amount of information carried by one of the signals given the samples of the other. Similar to normalized mutual information, the index is equal to zero when $x(n)$ and $y(n)$ are uncoupled, and is equal to one when the two processes are perfectly synchronized. In the case of the dual-axis vibration signals, the synchronization index measures the amount of information shared between the two axes about the two-dimensional position/movement of the hyoid and the larynx. In other words, the synchronization index reveals whether this position/movement is reflected in both directions or the movement is independent between the axes.

Protocol for Data Acquisition from Participants

Dual-axis vibration signals were collected from 50 consenting healthy adults (24 males, 26 females), ranging from 18 to 65 years of age (19 participants were 18–34 years old; 9 participants were 34-44 years old; 13 participants were 45–54 years old; and 9 participants were 55–65 years old). Participants were screened through a short survey outlining their medical history, and were excluded if they had any known or prior symptoms of swallowing difficulties, or if they had a history of stroke or other neurological conditions, head or neck cancer, neck or spinal injury or a tracheostomy. The study protocol was approved by the research ethics board of Bloorview Kids Rehab in Toronto, Canada.

After completing the medical history survey, participants were seated comfortably in a chair for the balance of the data collection. A dual-axis accelerometer (ADXL322, Analog Devices) was placed on the neck of each participant anterior to the cricoid cartilage and secured with double-sided tape. The two axes were positioned in the anterior–posterior (A–P) and superior–inferior (S–I) directions. Additionally, we collected signals from three other sensors: a triple-axis accelerometer (MMA7260Q, SparkFun Electronics) attached to a headband and centered on the participant's forehead to monitor head motions; a respiratory belt (1370G, Grass Technologies) secured around the participant's diaphragm to monitor breathing patterns; and a microphone placed 30 cm away from the participant's mouth to capture any vocalizations. These latter signals confirmed that the participants were indeed following the data collection protocol properly (i.e., only vocalizing when instructed). Based on experiences from previous studies[20,46] and in order to mimic the same hardware behavior, the signals acquired from the dual-axis accelerometer were band-pass filtered in hardware with a pass band of 0.1–3000 Hz and passed through an amplifier (P55, Grass Technologies). The amplified sensor data were collected with a sampling frequency of 10 kHz and synchronized in time with a LabVIEW program running on a computer, and stored on the hard drive for subsequent analyses as depicted in Fig. 1.

The data collection procedure included two primary conditions: a resting condition and an anaerobic condition. For the resting condition, the participants were asked to remain silent and motionless for 60 s. For the anaerobic condition, the participants were again asked to remain silent and motionless, as well as to stop

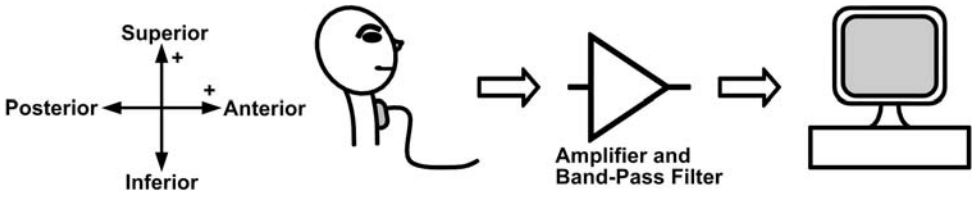

FIGURE 1. Data collection setup.

breathing for 10 s. In this case, we began recording data when the participants gave a hand signal indicating that they were ready to cease respiration. The participants also engaged in other tasks as a part of the data collection protocol for a different study. All participants were advised to refrain from swallowing during each task, but were permitted to swallow accumulated saliva between successive steps.

Data Acquisition for System Characterization

To characterize the baseline behavior of the data collection system, we used the same apparatus as in the previous section. However, the extra sensors used to monitor the participants' behavior were omitted. The dual-axis accelerometer was taped to a table in a vacant room in order to capture the system's exposure to random small vibrations. Ten recordings were made, each with a duration of approximately 60 s. These recordings were then used to approximately characterize the data collection system through the modeling technique described in "Mathematical Background" section.

Data Analysis

The first part of data analysis was concerned with modeling the data collection system using methods outlined in "Autoregressive Modeling of Data Acquisition System" section. The ten recordings, described in "Data Acquisition for System Characterization" section, were used for this purpose. Although the described protocol mandated 60 s of data, actual recordings were longer to facilitate removal of any transient behavior caused by human movement. Therefore, each recording was equally trimmed from both sides to generate 60-s recordings. Using these trimmed data, the AR modified covariance approach was used for system modeling. To determine the model order, Q, for each axis we examined various possible values ($Q \in \{1, 2, 3, \ldots, 1000\}$) using the BIC. The selected models were then used to annul the effects of instrumentation on the acquired data.

The second goal of this study was to examine the baseline stationarity and information-theoretic content of the dual-axis vibration signals. The recorded signals acquired from the participants were pre-processed with the inverse filters developed in the first part of the study. These filtered signals were then denoised using a 10-level discrete wavelet transform using the discrete Meyer wavelet with soft thresholding.[13,14] The pre-processed signals were then used for the baseline analysis. Baseline characterization proceeded with stationarity analysis, which was conducted according to the procedure outlined in "Statistical Characterization of Dual-Axis Cervical Accelerometry Signals" section. The number of segments was constrained to be at least 10 as a general rule of thumb for estimating a single statistical parameter. Given this constraint, the analysis was performed with varying window lengths. For both resting and anaerobic conditions, the window lengths were 1500, 3000, 5000, and 10,000 points, corresponding to temporal durations of 0.15, 0.3, 0.5 and 1 s given the sampling frequency of 10,000 Hz. The smallest window length was chosen based on the analysis of energy distribution using wavelet coefficients. It was found that on average more than 98% of the signal energy was retained below approximately 26 Hz implying that we require a window no shorter than 3.9 ms. Based on the recommendation made by Chau *et al.*,[7] we set the shortest window to be 0.15 s in duration and examined possible sources of nonstationarity for cases violating the stationarity hypothesis. Also, since the lengths of the acquired signals were not necessarily equal to an integer multiple of the window length, points from both ends of the signal were omitted as by Chau *et al.*[7] In addition to the stationary analysis outlined in "Statistical Characterization of Dual-Axis Cervical Accelerometry Signals" section, we characterized the frequency content of these baseline signals using three spectral features common to audio and biomedical signal analysis[22,30]:

- peak frequency

$$f_{\mathrm{p}} = \mathrm{argmax}_{f \in [0, f_{\max}]} |F_x(f)|^2 \tag{20}$$

- spectral centroid

$$\widehat{f} = \frac{\int_0^{f_{\max}} f |F_x(f)|^2 df}{\int_0^{f_{\max}} |F_x(f)|^2 df} \tag{21}$$

- the bandwidth

$$BW = \sqrt{\frac{\int_0^{f_{\max}} \left(f - \hat{f}\right)^2 |F_x(f)|^2 df}{\int_0^{f_{\max}} |F_x(f)|^2 df}}, \quad (22)$$

where $F_x(f)$ represents the Fourier transform of the signal, and $f_{\max}$ is the maximal analyzed frequency.

We also decomposed the identified nonstationary signals using a 10-level wavelet transform with the discrete Meyer wavelet. Our goal was to examine the effects of age and gender on the energy concentration at each decomposition level. The energy concentration was calculated using the wavelet coefficients as given by Lee *et al.*[20]

Next, we assessed the information-theoretic content of the dual-axis cervical vibration signals. To this end, we calculated the indexes of regularity and the synchronization using $\lambda = 10$ and $W = \{10, 11, 12, ..., 30\}$.

Using the Mann–Whitney test[26] and a weighted linear regression analysis, where appropriate, we tested for age and gender effects on the spectral and information-theoretic contents of baseline signals. These demographic variables reportedly influence actual swallowing signals.[8,46]

RESULTS AND DISCUSSION

Experimental Characterization of the Data Collection System

The results of system modeling are shown in Table 1. The model order for the A–P direction fluctuates between 8 and 9, while the model for the S–I direction is consistently a third order system. To ensure sufficient model complexity, a ninth-order model was chosen for the A–P direction. Hence, the average of ten transfer functions for the DAQ system in both directions are given by:

$$\begin{aligned} H_{\text{A-P}}(z) = 1/(1 &- 0.8850z^{-1} + 0.2983z^{-2} - 0.0445z^{-3} \\ &- 0.0018z^{-4} - 0.0095z^{-5} + 0.0205z^{-6} \\ &- 0.0220z^{-7} + 0.0156z^{-8} - 0.0071z^{-9}) \end{aligned} \quad (23)$$

TABLE 1. Model orders for A–P direction and S–I direction as determined by BIC.

Recording	I	II	III	IV	V	VI	VII	VIII	IX	X
A–P	8	8	9	9	9	9	9	9	8	8
S–I	3	3	3	3	3	3	3	3	3	3

$$H_{\text{S-I}}(z) = \frac{1}{1 - 0.8798z^{-1} + 0.2939z^{-2} - 0.0461z^{-3}}. \quad (24)$$

Note that even though the system hardware in both directions is identical, the above models are of different orders. A typical approach in system identification for model validation/comparison is to examine frequency responses of models for potential differences.[24] Amplitude and phase spectra for models given by (23) and (24) are depicted in Figs. 2(a) and 2(b), respectively. From these graphs, it can be concluded that the models for systems in the A–P (solid line) and S–I (dashed line) directions are practically identical. The higher model order in the A–P axis may be attributable to slowly evolving variations in the measured static gravitational acceleration. These slow fluctuations would result in higher estimated model orders due to the longer memory of the underlying process. On the other hand, the S–I axis, being aligned in a direction orthogonal to vertical, was not affected by static acceleration but only inertial accelerations. Hence, S–I model orders were consistently lower than corresponding A–P estimates. In addition, by examining the roots of both systems, we notice that the systems are stable: the poles are within the unit circle. Based on the transfer functions given by (23) and (24), an inverse filtering approach[9] was implemented to annul the effects of the data collection system. To demonstrate the effects of inverse filtering on the recordings, power spectral densities of a sample recording before processing are shown in Figs. 3(a) and 3(b). Their processed counterparts are depicted in Figs. 3(c) and 3(d). It is clear from these graphs that a recording with a pink-like spectrum on both axes becomes a recording with a white spectrum after inverse filtering. Whiteness of the filtered signals was checked using Lilliefors hypothesis test of composite normality.[23] All the recordings in the A–P and S–I directions ("Data Acquisition for System Characterization" section) became white sequences after processing with the inverse filters. This whitening filter is essential for subsequent study of swallowing accelerometry as the resultant signals now reflect true baseline characteristics of cervical vibrations, without any contaminating effects of the implemented hardware.

Baseline Characterization of Dual-Axis Swallowing Accelerometry Signals

The results of the stationarity analysis for the two conditions are summarized in Table 2. Approximately 50% of the baseline dual-axis cervical vibration signals were weakly stationary in nature. The number of

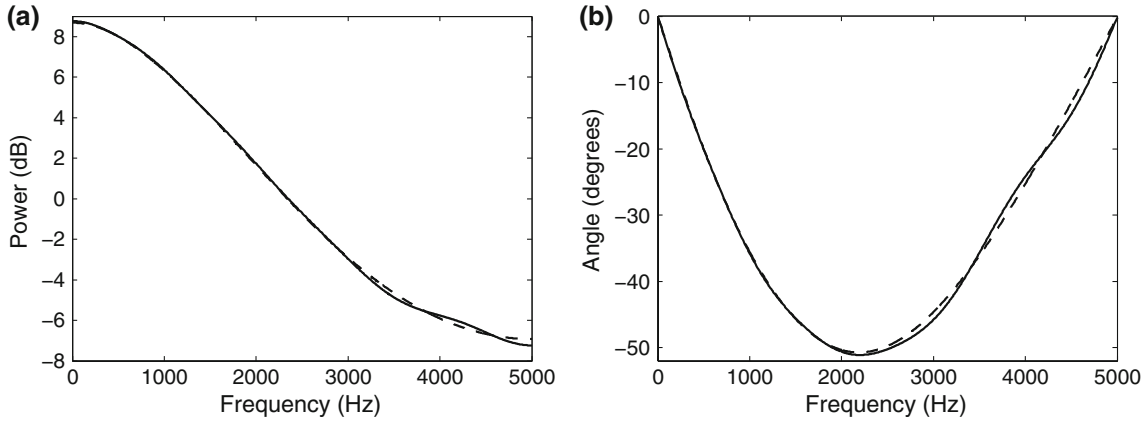

FIGURE 2. Modeling of the data acquisition system: (a) amplitude and (b) phase spectra of the models.

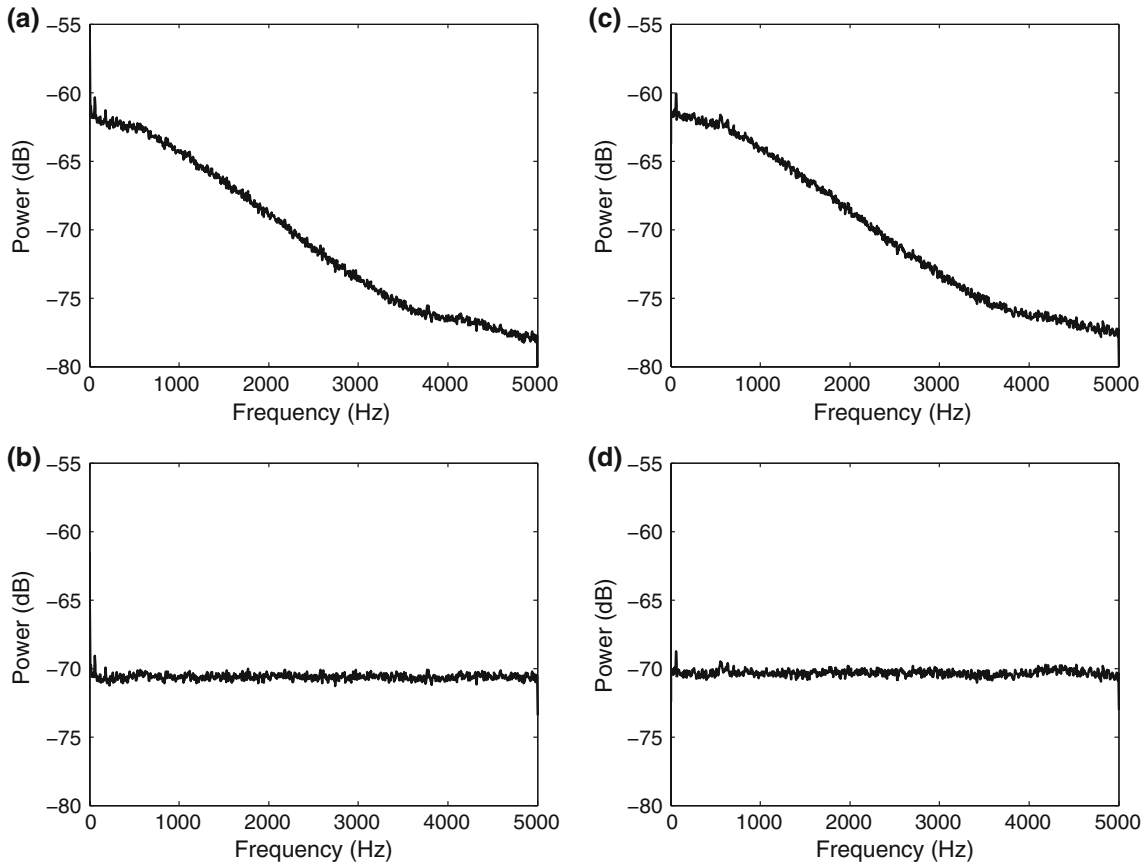

FIGURE 3. Effects of inverse filtering. Power spectra in (a) the A–P and (b) the S–I directions for a sample signal prior to inverse filtering. Power spectra in (c) the A–P and (d) the S–I directions after inverse filtering.

nonstationary signals was approximately equal for both conditions, implying that nonstationarities in swallowing vibration signals are likely not attributable to respiration. Accordingly, future developments in swallowing vibration will not require an algorithm to mitigate respiratory vibrations, although such filtering is required in other biomedical applications.[50] As the length of the analyzing window increases, there were fewer nonstationarities, as expected. The values of the stationarity test statistic, ρ_{Ω}, were statistically equivalent regardless of the window length for the resting condition (Kruskal–Wallis test: $p_{\mathrm{A-P}} = 0.97$, $p_{\mathrm{S-I}} = 0.96$). When considering the anaerobic condition, the test statistic values were only statistically

TABLE 2. Stationarity analysis of dual-axis swallowing vibration recordings during the resting and anaerobic conditions.

	Resting condition			Anaerobic condition		
Window length	A–P	S–I	# Segments	A–P	S–I	# Segments
0.15 s	35 (70)	29 (58)	420 ± 17	38 (76)	32 (64)	81 ± 8
0.3 s	31 (62)	22 (44)	209 ± 9	35 (70)	31 (62)	40 ± 4
0.5 s	29 (58)	20 (40)	126 ± 6	26 (52)	25 (50)	24 ± 2
1 s	27 (54)	16 (32)	63 ± 3	18 (36)	21 (42)	12 ± 1

Columns denoted by A–P and S–I show the number (percentage) of nonstationary signals in the respective direction.

TABLE 3. Frequency analysis of dual-axis swallowing vibration recordings during the resting test.

	A–P direction			S–I direction		
	f_p	$\hat{f}$	*BW*	f_p	$\hat{f}$	*BW*
Overall	0.31 ± 0.14	4.32 ± 3.42	10.6 ± 4.78	1.78 ± 2.65	12.9 ± 6.70	14.8 ± 6.69
Male	0.39 ± 0.28	2.86 ± 1.96	8.81 ± 3.85	2.75 ± 3.99	12.6 ± 6.89	14.4 ± 7.64
Female	0.22 ± 0.05	5.65 ± 4.47	12.2 ± 4.83	0.88 ± 1.18	13.2 ± 6.58	15.2 ± 5.63
$18 < Age < 35$	0.23 ± 0.06	6.17 ± 4.45	12.9 ± 4.72	2.39 ± 3.86	17.9 ± 5.23	14.7 ± 3.45
$35 \le Age < 45$	0.24 ± 0.03	3.62 ± 3.56	8.75 ± 3.50	2.85 ± 4.64	11.9 ± 8.21	11.4 ± 5.66
$45 \le Age < 55$	0.48 ± 0.50	3.27 ± 2.26	11.0 ± 4.63	0.69 ± 0.82	8.71 ± 3.91	14.1 ± 6.42
$55 \le Age < 65$	0.25 ± 0.05	2.61 ± 2.09	7.00 ± 2.70	1.00 ± 1.10	9.36 ± 6.38	19.7 ± 16.5

Entries are mean values ± mean average deviations in Hz.

TABLE 4. Frequency analysis of dual-axis swallowing vibration recordings during the anaerobic test.

	A–P direction			S–I direction		
	f_p	$\hat{f}$	*BW*	f_p	$\hat{f}$	*BW*
Overall	0.36 ± 0.41	7.13 ± 5.19	30.9 ± 22.1	5.12 ± 6.10	13.3 ± 5.73	21.9 ± 12.6
Male	0.57 ± 0.70	7.01 ± 5.92	27.4 ± 19.5	5.72 ± 5.70	13.1 ± 5.83	23.9 ± 16.2
Female	0.16 ± 0.11	7.24 ± 4.50	34.1 ± 24.5	4.57 ± 6.25	13.5 ± 5.68	20.1 ± 9.60
$18 < Age < 35$	0.20 ± 0.15	9.01 ± 6.69	29.2 ± 18.9	9.73 ± 8.96	18.0 ± 5.22	24.2 ± 13.2
$35 \le Age < 45$	0.26 ± 0.22	6.36 ± 5.08	29.1 ± 19.1	4.51 ± 5.00	11.9 ± 6.20	17.3 ± 6.93
$45 \le Age < 55$	0.25 ± 0.26	4.99 ± 3.38	34.9 ± 21.8	1.11 ± 1.40	11.0 ± 3.25	23.0 ± 15.2
$55 \le Age < 65$	0.96 ± 1.43	7.04 ± 4.66	30.4 ± 30.6	1.82 ± 2.52	8.17 ± 3.87	20.1 ± 14.5

Entries are mean values ± mean average deviations in Hz.

equal for window lengths greater than 0.5 s (Mann–Whitney test: $p_{A-P} = 0.38$, $p_{S-I} = 0.10$). To examine the source of nonstationarities, a window length of 0.5 s was chosen, since ρ_Ω values stabilized at this window size for both conditions. The vast majority of nonstationary signals had time-varying mean, variance, and median frequency. To further understand the physiological sources of (non)stationarity, we conducted a frequency analysis of all signals as described in "Data Analysis" section. Tables 3 and 4 only depict the results for the three extracted frequency features, since the wavelet analysis of nonstationary recordings revealed no age- or gender-related effects. Several observations are in order. First, there are no gender-based statistical differences between the results. That is, given a specific test (e.g., resting or anaerobic) and a specific direction (e.g., A–P or S–I) the frequency content does not statistically differ between male and female participants ($p > 0.05$ for f_p, $\hat{f}$ and *BW* in both A–P and S–I directions and in both resting and anaerobic conditions). Second, age does not seem to uniformly affect the frequency content of the baseline recordings. For example, in the resting condition, the bandwidth in the A–P direction and the peak frequency in the S–I directions were affected by age ($p \le 0.02$, regression test) while in the anaerobic condition, the peak frequency in the S–I direction exhibited an age dependence ($p \le 10^{-4}$, regression test). Additionally, the age related effects were observed even when we split the recordings into stationary and

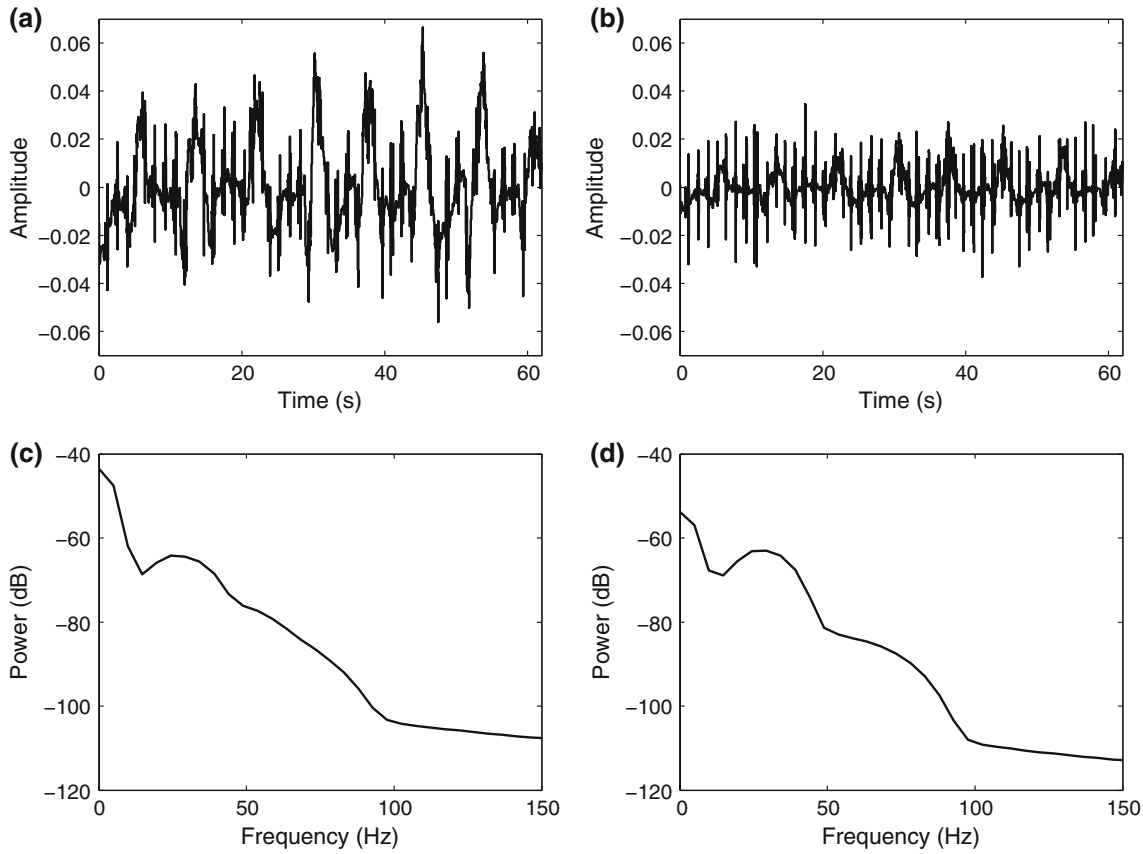

FIGURE 4. Sample signals in (a) the A–P and (b) the S–I directions during the resting test. Power spectra in (c) the A–P and (d) the S–I directions for the sample recordings. The values of measured features for these two recordings are: $f_{p_{AP}} = 0.13$ Hz, $f_{p_{SI}} = 0.13$ Hz, $\hat{f}_{AP} = 1.24$ Hz, $\hat{f}_{SI} = 7.50$ Hz, $BW_{AP} = 5.73$ Hz, $BW_{SI} = 12.3$ Hz, $\varrho_{AP} = 9.99 \times 10^{-1}$, $\varrho_{SI} = 9.99 \times 10^{-1}$, $\eta_{AP-SI} = 0.89$.

nonstationary groups. Third, the maximum power in the A–P direction occurred at very low frequencies. Based on these findings, we anticipate that nonstationarities and variations in the frequency content are due to the fact that the dual-axis cervical accelerometry is capturing information related to cardiac dynamics (see Fig. 4). The superior thyroid artery outlines the lateral aspect of the thyroid cartilage, where we positioned our accelerometer. In particular, we speculate that vasomotion of the common carotid artery and its branches, i.e., the external carotid and superior thyroid artery, is responsible for the observed maximum power occurring at low frequencies. Previous literature has reported similar frequency content for vasomotion.[10,44] Additional auditory examination of the baseline signals revealed the presence of vibrations associated with heart beats and blood flow (see Fig. 4). Studies implementing similar auscultatory techniques[21] reported comparable findings. Note that for the cases where age affects the frequency content, there is a decreasing trend, i.e., older participants exhibit slower vibrations. This also suggests that the observed vibrations in the baseline state are related to heart rate variation, as it decreases with age.[31] As a last remark, we must also acknowledge the potential effect of respiration on these signals.[38] To fully understand these potential effects, future studies should compare dual-axis cervical vibration signals with direct recordings of peripheral resistance changes and respiration via statistical analysis (e.g., coherence analysis).

The assessment of the information-theoretic content of the baseline signals is in Table 5. Several observations are in order. First, the baseline signals in both resting and anaerobic conditions are highly regular. The index of regularity is almost one for all the cases, and the standard deviations are close to zero (Table 5, columns 1, 2, 4, and 5). This finding is expected, since Tables 3 and 4 show a very structured behavior of signals in the frequency domain. Second, gender does not influence the information content of the baseline characteristics of dual-axis cervical vibration signals. There was no gender effect on the index of regularity for both resting ($p_{AP} = 0.14$, $p_{SI} = 0.65$) and anaerobic conditions ($p_{AP} = 0.26$, $p_{SI} = 0.42$). Similarly, the synchronization index between the A–P and S–I axes did not exhibit any association with gender ($p_{resting} = 0.48$, $p_{anaerobic} = 0.52$). Previous research has shown that there are gender-based swallowing

TABLE 5. Information-theoretic content of dual-axis swallowing vibration baseline recordings (ϱ = the index of regularity, η = the synchronization index).

	Resting test			Anaerobic test		
	ϱ_{AP}	ϱ_{SI}	η_{AP-SI}	ϱ_{AP}	ϱ_{SI}	η_{AP-SI}
Overall	9.99 ± 0.00	9.99 ± 0.00	8.48 ± 1.43	9.98 ± 0.00	9.98 ± 0.00	8.78 ± 1.04
Male	9.99 ± 0.00	9.99 ± 0.00	8.68 ± 1.22	9.98 ± 0.00	9.98 ± 0.00	8.89 ± 0.98
Female	9.99 ± 0.00	9.99 ± 0.00	8.29 ± 1.59	9.99 ± 0.00	9.99 ± 0.00	8.68 ± 1.10
$18 < Age < 35$	9.99 ± 0.00	9.99 ± 0.00	8.22 ± 1.81	9.98 ± 0.00	9.98 ± 0.00	8.62 ± 1.08
$35 \leq Age < 45$	9.99 ± 0.00	9.99 ± 0.00	8.64 ± 1.19	9.98 ± 0.00	9.98 ± 0.00	9.26 ± 0.76
$45 \leq Age < 55$	9.99 ± 0.00	9.99 ± 0.00	8.55 ± 1.16	9.98 ± 0.00	9.98 ± 0.00	9.06 ± 0.92
$55 \leq Age < 65$	9.99 ± 0.00	9.99 ± 0.00	8.77 ± 1.19	9.99 ± 0.00	9.98 ± 0.00	8.23 ± 1.18

All presented values should be multiplied by 10^{-1}.

differences due to anatomical differences in the oropharyngeal mechanism.[8,46] Hence, the results presented here are important as they demonstrate that such gender-based differences do not exist in baseline accelerometry, when there is no swallowing involved. Similarly, the age of the participant did not influence the information content of the baseline recording. Regardless of the age of the participant, the information unique to each axis or shared between A–P and S–I directions is statistically equivalent ($p > 0.4$, regression test). However, we know that the length of time required for a person to complete a swallow increases with age, due to the decoupling of the oral and pharyngeal stages.[46,49] It therefore appears that both age and gender related effects on cervical vibrations only manifest themselves during actual swallowing activity and not during baseline resting and anaerobic conditions.

Remarks

The current manuscript has only described the baseline characteristics of dual-axis cervical vibration signals obtained from a healthy population and has not considered populations with dysphagia. Swallowing difficulties may be secondary to numerous distinct conditions, such as stroke, acquired brain injury, advanced aging, or head and neck cancers, among others. Hence, we may expect to see some differences in baseline signals, particularly for individuals who may have concomitant cariorespiratory conditions. However, it is also plausible that the resting and anaerobic characteristics of cervical vibration signals of these patient populations may actually resemble those of the healthy population studied here. Keep in mind that the baseline conditions do not invoke swallowing function, which is the distinguishing characteristic between the healthy and pathological populations of interest. Clearly, future studies with different populations of individuals with dysphagia are necessary to test these hypotheses. Nonetheless, this study has provided an understanding of normative baseline characteristics. This knowledge may eventually be helpful for differentiating between healthy and abnormal populations, particularly, in gauging the need to remove baseline effects from signals prior to patient classification.

CONCLUSION

In this paper, baseline characteristics of dual-axis vibration signals were studied. The DAQ system itself was modeled using an AR approach, and consistent models were determined for the two axes. Based on these models, the inverse filtering annulled the effects introduced by instrumentation. The study of the baseline characteristics revealed that approximately half of the acquired dual-axis swallowing cervical signals are stationary. Also, there exists some dependence between the two axes. Low-frequency oscillations detected in these recordings may be attributed to vasomotion of blood vessels in proximity of the thyroid cartilage. Statistical analysis demonstrated that information-theoretic characteristics of baseline vibration signals are generally not affected by age and gender. However, some spectral characteristics experience an age-related dependence.

ACKNOWLEDGMENTS

This research was funded in part by the Ontario Centres of Excellence, the Toronto Rehabilitation Institute, Bloorview Kids Rehab, and the Canada Research Chairs Program.

REFERENCES

[1]Akaike, H. A new look at the statistical model identification. *IEEE Trans. Autom. Contr.* 19(6):716–723, 1974.

[2]Alves, N., and T. Chau, Stationarity distributions of mechanomyogram signals from isometric contractions of extrinsic hand muscles during functional grasping. *J. Electromyogr. Kinesiol.* 18(3):509–515, 2008.
[3]Barron, A., J. Rissanen, and B. Yu, The minimum description length principle in coding and modeling. *IEEE Trans. Inf. Theory*, 44(6):2743–2760, 1998.
[4]Bendat, J. S., and A. G. Piersol. Random Data: Analysis and Measurement Procedures, 2nd edn. New York, NY: Wiley, 1986.
[5]Brockwell, P. J., and R. A. Davis., Time Series: Theory and Methods, 2nd ed. New York, NY: Springer-Verlag, 1991.
[6]Cao, H., B. R. Ellis, and J. D. Littler, The use of the maximum entropy method for the spectral analysis of wind-induced data recorded on buildings. *J. Wind Eng. Industr. Aerodyn.* 72:81–93, 1997.
[7]Chau, T., D. Chau, M. Casas, G. Berall, and D. J. Kenny, Investigating the stationarity of paediatric aspiration signals. *IEEE Trans. Neural Syst. Rehabil. Eng.* 13(1):99–105, 2005.
[8]Cichero, J. A. Y. and B. E. Murdoch. Acoustic signature of the normal swallow: characterization by age, gender, and bolus volume. *Ann. Otol. Rhinol. Laryngol.* 111(7 Pt 1):623–632, 2002.
[9]Clancy, E. A., and N. Hogan. Single site electromyograph amplitude estimation. *IEEE Trans. Biomed. Eng.* 41(2):159–167, 1994.
[10]Colantuoni, A., S. Bertuglia, and M. Intaglietta. Quantitation of rhythmic diameter changes in arterial microcirculation. *Am. J. Physiol. Heart Circ. Physiol.* 246(4):508–517, 1984.
[11]Cover, T. M., and J. A. Thomas. Elements of Information Theory, Wiley Series in Telecommunications. New York, NY: Wiley, 1991.
[12]Das, A., N. P. Reddy, and J. Narayanan, Hybrid fuzzy logic committee neural networks for recognition of swallow acceleration signals. *Comput. Meth. Progr. Biomed.* 64(2):87–99, 2001.
[13]Donoho, D. L. De-noising by soft-thresholding. *IEEE Trans. Inf. Theory*, 41(3):613–627, 1995.
[14]Donoho, D. L., and I. M. Johnstone. Ideal spatial adaptation by wavelet shrinkage. *Biometrika* 81(3):425–455, 1994.
[15]Ishida, R., J. B. Palmer, and K. M. Hiiemae, Hyoid motion during swallowing: factors affecting forward and upward displacement. *Dysphagia*, 17(4):262–272, 2002.
[16]Kay, S. M. Modern Spectral Estimation: Theory and Application. Englewood Cliffs, NJ: Prentice Hall, 1988.
[17]Kay, S. M., and S. L. Marple, Spectrum analysis—a modern perspective. *Proc. IEEE* 69(11): 1380–1419, 1981.
[18]Kim, Y., and G. H. McCullough, Maximum hyoid displacement in normal swallowing. *Dysphagia* 23(3):274–279, 2008.
[19]Lee, J., S. Blain, M. Casas, D. Kenny, G. Berall, and T. Chau. A radial basis classifier for the automatic detection of aspiration in children with dysphagia. *J. NeuroEng. Rehabil.* 3:14, 2006. doi:10.1186/1743-0003-3-14.
[20]Lee, J., C. M. Steele, and T. Chau, Time and time-frequency characterization of dual-axis swallowing accelerometry signals. *Physiol. Measure* 29(9):1105–1120, 2008.
[21]Lees, R. S. Phonoangiography: qualitative and quantitative. *Ann. Biomed. Eng.* 12(1):55–62, 1984.
[22]Li, S. Z. Content-based classification and retrieval of audio using the nearest feature line method. *IEEE Trans. Speech Audio Process.* 8(5):619–625, 2000.
[23]Lilliefors, H. W. On the Kolmogorov–Smirnov test for normality with mean and variance unknown. *J. Am. Stat. Assoc.* 62(318):399–402, 1967.
[24]Ljung, L. System Identification: Theory for the User, 2nd edn. Upper Saddle River, NJ: Prentice-Hall, 1999.
[25]Logemann, J. A. Evaluation and Treatment of Swallowing Disorders, 2nd ed. Austin, TX: PRO-ED, 1998.
[26]Mann, H. B., and D. R. Whitney, On a test of whether one of two random variables is stochastically larger than the other. *Ann. Math. Stat.* 18(1):50–60, 1947.
[27]Marple, L. A new autoregressive spectrum analysis algorithm. *IEEE Trans. Acoust.* 28(4):441–454, 1980.
[28]Marple, S. L. *Digital Spectral Analysis: With Applications*. Englewood Cliffs, NJ: Prentice-Hall, Inc., 1987.
[29]McConaghy, T., H. Leung, E. Bossé, and V. Varadan, "Classification of audio radar signals using radial basis function neural networks," *IEEE Trans. Instrum. Measure.* 52(6):1771–1779, 2003.
[30]Merletti, R., A. Gulisashvili, and L. R. Lo Conte. Estimation of shape characteristics of surface muscle signal spectra from time domain data. *IEEE Trans. Biomed. Eng.* 42(8):769–776, 1995.
[31]O'Brien, I. A., P. O'hare, and R. J. Corrall, Heart rate variability in healthy subjects: effect of age and the derivation of normal ranges for tests of autonomic function. *Brit. Heart J.* 55(4):348–354, 1986.
[32]Paiss, O., and G. F. Inbar, Autoregressive modeling of surface EMG and its spectrum with application to fatigue. *IEEE Trans. Biomed. Eng.* 34(10):761–770, 1987.
[33]Papoulis, A. Probability, Random Variables, and Stochastic Processes, 3rd edn. New York: WCB/McGraw-Hill, 1991.
[34]Porta, A., G. Baselli, D. Liberati, N. Montano, C. Cogliati, T. Gnecchi-Ruscone, A. Malliani, and S. Cerutti, Measuring regularity by means of a corrected conditional entropy in sympathetic outflow. *Biol. Cybernet.* 78(1):71–78, 1998.
[35]Porta, A., G. Baselli, F. Lombardi, N. Montano, A. Malliani, and S. Cerutti, Conditional entropy approach for the evaluation of the coupling strength. *Biol. Cybernet.* 81(2):119–129, 1999.
[36]Porta, A., S. Guzzetti, N. Montano, R. Furlan, M. Pagani, A. Malliani, and S. Cerutti, Entropy, entropy rate, and pattern classification as tools to typify complexity in short heart period variability series. *IEEE Trans. Biomed. Eng.* 48(11):1282–1291, 2001.
[37]Porta, A., S. Guzzetti, N. Montano, M. Pagani, V. Somers, A. Malliani, G. Baselli, and S. Cerutti, Information domain analysis of cardiovascular variability signals: Evaluation of regularity, synchronisation and co-ordination. *Med. Biol. Eng. Comput.* 38(2):180–188, 2000.
[38]Porta, A., E. Tobaldini, S. Guzzetti, R. Furlan, N. Montano, and T. Gnecchi-Ruscone. Assessment of cardiac autonomic modulation during graded head-up tilt by symbolic analysis of heart rate variability. *Am. J. Physiol. Heart Circ. Physiol.* 293(1):H702–H708, 2007.
[39]Ramsey, D. J. C., D. G. Smithard, and L. Kalra, Can pulse oximetry or a bedside swallowing assessment be used to detect aspiration after stroke? *Stroke*, 37(12): 2984–2988, 2006.
[40]Reddy, N. P., E. P. Canilang, J. Casterline, M. B. Rane, A. M. Joshi, R. Thomas, and R. Candadai, Noninvasive accelaration measurements to characterize the pharyngeal phase of swallowing. *J. Biomed. Eng.* 13:379–383, 1991.

[41]Reddy, N. P., B. R. Costarella, R. C. Grotz, and E. P. Canilang, Biomechanical measurements to characterize the oral phase of dysphagia. *IEEE Trans. Biomed. Eng.* 37(4):392–397, 1990.

[42]Reddy, N. P., A. Katakam, V. Gupta, R. Unnikrishnan, J. Narayanan, and E. P. Canilang, Measurements of acceleration during videofluorographic evaluation of dysphagic patients. *Med. Eng. Phys.* 22(6):405–412, 2000.

[43]Rissanen, J. Modeling by shortest data description. *Automatica*, 14(5):465–471, 1978.

[44]Schmidt-Lucke, C., P. Borgström, and J. A. Schmidt-Lucke. Low frequency flowmotion/(vasomotion) during patho-physiological conditions. *Life Sci.* 71(23): 2713–2728, 2002.

[45]Schwarz, G. Estimating the dimension of a model. *Ann. Stat.* 6(2):461–464, 1978.

[46]Sejdić, E., C. M. Steele, and T. Chau, Segmentation of dual-axis swallowing accelerometry signals in healthy subjects with analysis of anthropometric effects on duration of swallowing activities. *IEEE Trans. Biomed. Eng.* 56(4): 1090–1097, 2009.

[47]Steele, C., C. Allen, J. Barker, P. Buen, R. French, A. Fedorak, S. Day, J. Lapointe, L. Lewis, C. MacKnight, S. McNeil, J. Valentine, and L. Walsh, Dysphagia service delivery by speech-language pathologists in Canada: results of a national survey. *Can. J. Speech-Language Pathol. Audiol.* 31(4):166–177, 2007.

[48]Stoica, P., and Y. Selén, Model-order selection: a review of information criterion rules. *IEEE Signal Process. Mag.* 21(4):36–47, 2004.

[49]Tracy, J. F., J. A. Logemann, P. J. Kahrilas, P. Jacob, M. Kobara, and C. Krugler. Preliminary observations on the effects of age on oropharyngeal deglutition. *Dysphagia* 4(2):90–94, 1989.

[50]Wang, P., Y. Kim, L. H. Ling, and C. B. Soh, First heart sound detection for phonocardiogram segmentation. In: Proc. of 27th Annual International Conference of the Engineering in Medicine and Biology Society (IEEE-EMBS 2005), Shanghai, China, Sept. 1–5, 2005, pp. 5519–5522.

[51]Yang, Y. Can the strengths of AIC and BIC be shared? A conflict between model indentification and regression estimation. *Biometrika* 92(4):937–950, 2005.